



HAL
open science

Evaluation of airborne and satellite electro-optical sensors performances by use of high-altitude clouds occurrence climatology.

K. Caillault, A. Bizard, C. Lavigne, A. Roblin, P. Chervet

► **To cite this version:**

K. Caillault, A. Bizard, C. Lavigne, A. Roblin, P. Chervet. Evaluation of airborne and satellite electro-optical sensors performances by use of high-altitude clouds occurrence climatology.. 6th International Symposium on Optronics in Defence and Security (OPTRO 2014), Jan 2014, PARIS, France. hal-01059047

HAL Id: hal-01059047

<https://onera.hal.science/hal-01059047>

Submitted on 29 Aug 2014

HAL is a multi-disciplinary open access archive for the deposit and dissemination of scientific research documents, whether they are published or not. The documents may come from teaching and research institutions in France or abroad, or from public or private research centers.

L'archive ouverte pluridisciplinaire **HAL**, est destinée au dépôt et à la diffusion de documents scientifiques de niveau recherche, publiés ou non, émanant des établissements d'enseignement et de recherche français ou étrangers, des laboratoires publics ou privés.

EVALUATION OF AIRBORNE AND SATELLITE ELECTRO-OPTICAL SENSORS PERFORMANCES BY USE OF HIGH-ALTITUDE CLOUDS OCCURRENCE CLIMATOLOGY

OECD CONFERENCE CENTER, PARIS, FRANCE / 28–30 JANUARY 2014

K. Caillault⁽¹⁾, A. Bizard⁽¹⁾, C. Lavigne⁽¹⁾, A. Roblin⁽¹⁾, P. Chervet⁽¹⁾

⁽¹⁾ *Onera – The French Aerospace Lab, F-91761 Palaiseau, France,*
email : karine.caillault@onera.fr

KEYWORDS: sensor performance, climatology, high altitude cloud

ABSTRACT:

Remote sensing, surveillance applications or telecommunications require optronic sensors, onboard satellite or airborne platform. Performances limitation of these sensors may be caused by cloud presence in the field of view. To take into account cloud presence, a Monte Carlo method is used. Geometrical and optical clouds properties necessary to build the model are obtained from CALIOP measurements that enable one to deal with the optically thinnest clouds. Different viewing geometries are presented. They correspond to surveillance missions by an airborne sensor with close-to-the-horizon viewing and to optical link between an aircraft and a satellite. Results obtained are compared to a previous study and improvements reached with our new method are discussed.

1. INTRODUCTION

The impact of high-altitude clouds along an electro-optical sensor line of sight has been studied for various applications such as hot sources detection in the infrared domain [1] or laser transmission [2-3]. Clouds can either produce an attenuation of the target signal or an increase in background radiation due to thermal emission or sun light scattering. Statistical aspects of cloud occurrence have to be considered. Getting transmittance statistics is also an important challenge to a number of applications such as ballistic missile defence, ground data collection, laser communications and detection of targets through the atmosphere.

Estimation of the probability of a Cloud Free Line of Sight (CFLOS), i.e. the ability to obtain a LOS through the atmosphere unimpeded by cloud presence, has been widely documented [4-9] for applications such as laser communications or missile defence. Clouds statistics taken into account in these studies rely on data from passive

meteorological sensors which provide a reasonable measurement of cloud top altitudes, but do not provide information about cloud bases or multi-layered clouds [10-12]. Moreover they are not sensitive enough to detect the thinnest clouds that can be numerous at high altitudes.

Spaceborne observations from satellites flying together with complementary instruments, namely the A-TRAIN, offer now new opportunities to provide an unprecedented survey of cloud properties on a global scale [13] and to compile more reliable representations of clouds to accurately estimate transmittance statistics. Cloud-Aerosol Lidar and Infrared Pathfinder Satellite Observations (CALIPSO), a joint U.S. National Aeronautics and Space Administration (NASA) and French Centre National d'Etudes Spatiales (CNES) satellite mission, launched in April 2006, is dedicated to the study of aerosols and thin clouds (with a detection limit as low as 0.01 in term of optical depth) [14-18]. The payload includes Cloud-Aerosol Lidar with Orthogonal Polarization (CALIOP), which delivers for the first time on a global scale, multi-year measurements of vertical profiles of clouds and aerosols backscattering properties.

Transmittance statistics only based on CFLOS may be too restrictive to predict the chance for mission success. Indeed, the detection performance of a satellite or airborne optronic sensor can vary widely as a function of local meteorology and viewing geometry. Getting transmittance statistics is thus necessary. The degree of atmosphere transparency for which a mission is supposed to be successful is given by a transmittance threshold, above which atmosphere is considered to be clear enough to obtain good detection performances.

With this study, we aim to determine transmittance statistics for various LOS configurations with several transmittance thresholds. Seasonal variation is also taken into account and the assumption of horizontally infinitely wide clouds is tested versus finite length clouds. Transmittance statistics are calculated by use of high clouds properties (called climatology thereafter) obtained

from CALIOP products.

The paper is organized as follows. In section 2, the high-cloud occurrence climatology obtained from CALIOP products is presented and the methodology used to calculate transmittance probabilities is described. In section 3, sensor performances calculations are presented for two main applications: (1) surveillance mission by an airborne sensor (close-to-the-horizon viewing angle / oblique viewing angle), and (2) optical link between a satellite and an airborne sensor. Concluding remarks are given in section 4.

2. TRANSMITTANCE PROBABILITIES FROM HIGH-ALTITUDE CLOUDS OCCURRENCE CLIMATOLOGY

2.1. High-altitude clouds occurrence climatology

Long-term global cloud climatologies have been derived from a number of different passive satellite sensors: the imaging radiometer MODerate resolution Imaging Spectroradiometer (MODIS) [19], the suite of weather satellites giving radiance measurements for the International Satellite Cloud Climatology Project (ISCCP) [20], the Stratospheric Aerosol and Gas Experiment II (SAGEII) photometer [21]. The main limitations of these instruments are an optical depth detection limit greater than 0.3 which prevents detection of optically thin clouds and the lack of information about cloud bases or multi-layered clouds. Infrared vertical sounders such as Television InfraRed Observation Satellite (TIROS-N) Operational Vertical Sounder (TOVS) [22] are more sensitive to low optical depth clouds with a detection limit at 0.1 [10][23]. This detection limit is still too high to detect subvisible clouds (optical depth < 0.03) and a large part of semitransparent clouds (0.03 < optical depth < 0.3). These cloud classes, defined in [24] as well as the opaque clouds class with optical depth greater than 0.3, are widely used in papers relative to high-cloud studies. However, for the sake of clarity concerning our study, we propose to add a "thick cloud" category with optical depth between 0.3 and 3. The "opaque" category will only cover clouds with optical depth higher than 3 for which transmittance is smaller than 0.05. Active optical sensors can reach optical depth detection limit as low as 0.01 [25] and several cloud climatologies from ground lidars have been established over time. However, the measurements are local ([18][26-28]) and affected by presence of low clouds [29].

CALIOP products have been selected to build the high-clouds climatology required for transmittance statistics calculation, thanks to an optical depth detection limit at 0.01 or less with sufficient averaging [15][30], a global coverage and a multi-year collection. CALIPSO spacecraft follows a sun-synchronous orbit passing in the same track every 16 days [15]. CALIOP is a two-wavelength depolarization lidar (532 and 1064 μm). Detection

of cloud layers primarily relies on the 532 μm channel and is based on an adaptive threshold detection technique [31]. Vertical resolution is 30 m from 0 to 8.2 km altitude, 60 m from 8.2 to about 20.2 km and 180 m above 20.2 km. CALIOP level 2 (version 3.01) data products are used in this study [32]. Cloud properties are obtained from CALIOP cloud layer products at 5 km resolution (L2 5 km). These layer properties specify the spatial and optical characteristics of each feature found and include quantities such as layer base and top altitudes, integrated attenuated backscatter and optical depth cloud. Comparisons of CALIOP observations with ground-based or airborne lidar measurements show an overall good agreement despite discrepancies in cloud fraction retrieval [18][33-34]. We use both CALIOP daytime and nighttime data products from June 2006 to September 2011. The climatology is built on a $3^\circ \times 3^\circ$ horizontal resolution grid with global coverage (latitude: 80°N - 80°S ; longitude 180°W - 180°E) and a 2 km vertical resolution. Cloud occurrences are calculated as a function of cloud altitude, optical depth and geometric thickness. Only clouds with tops higher than 7 km are taken into account in our climatology consistent with the surveillance applications and the associated viewing conditions. As an example of our climatology, Fig. 1 shows occurrences of clouds with optical depth higher than 0.3, in the range of cloud top altitudes 11-13 km, in spring, at nighttime.

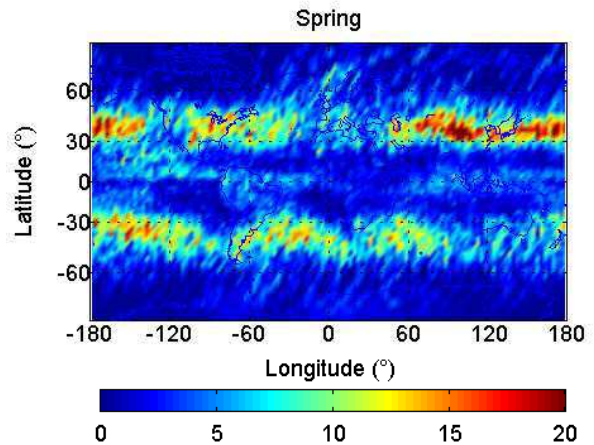


Figure 1. Occurrences of clouds (%) with optical depth > 0.3, with top height between 11 and 13 km, in spring, during nighttime, from CALIOP.

2.2. Transmittance probabilities

Transmittance probabilities from high-clouds occurrence climatology is required to get statistical evaluation of airborne or satellite sensors performances. In this study, we suppose that extinction is only due to clouds, that is aerosols and molecular extinction are not considered.

Cloud transmittance T along the sensor LOS is given by $T = e^{-\tau}$. τ is the cloud optical depth and can be written as $\tau = \sum_i \sigma_i l_i$ where i is the i^{th} crossed cloud layer, σ_i is the extinction coefficient

of cloud layer i , l_i is the length of the LOS segment crossing cloud layer i . The viewing geometry for an airborne sensor at altitude H , with viewing angle θ , is given in Fig. 2.

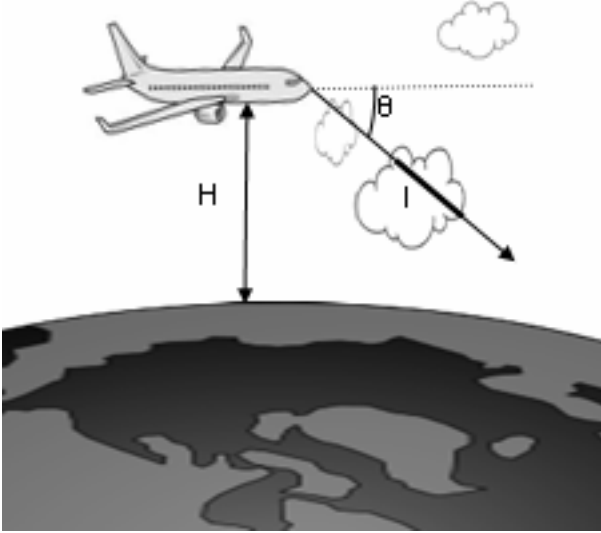


Figure 2. Viewing geometry of an airborne sensor at height H , with viewing angle θ . l is the segment of the sensor LOS crossing the cloud layer.

In order to get transmittance statistics, one needs to estimate the clouds joint probability density $P(x_1, x_2, x_3)$. It is the probability of cloud presence at altitude i , with geometrical thickness dl and optical depth dr . Its expression is:

$$P(x_1, x_2, x_3) = \frac{\sum N(x_1, x_2, x_3)}{N_T} \quad (1)$$

where x_1 stands for cloud height, x_2 for optical depth and x_3 for geometrical thickness, $N(x_1, x_2, x_3)$ is the number of samplings meeting selected values of x_1 , x_2 and x_3 , N_T is the total number of cloudy samplings, whatever the cloud height, optical depth and geometrical thickness.

As there is no information about cloud length, clouds are considered to be horizontally infinitely wide in a first step, that will be called *infinite* cloud case.

A more realistic cloud model can be defined by use of finite rectangles. In that case, cloud horizontal extent is required. Reference [35] gives statistics of high-clouds horizontal extent. They are established from 4-years ground-based measurements at the COVE station (37°N; 75°W): horizontal spatial extent is smaller than 50 km for 39% of high clouds, ranges between 50 and 100 km for 23%, ranges between 100 et 200 km for 16% and is greater than 200 km for 22%. Despite the lack of representativeness of these statistics at the global scale, we use them to get data to create a finite cloud model. Since these cloud lengths statistics relative to high-clouds do not depend on cloud altitude, joint probability density including cloud

horizontal length can be written as:

$$P(x_1, x_2, x_3, x_4) = P(x_1, x_2, x_3) \times P(x_4) \quad (2)$$

where x_4 stands for cloud length and

$$P(x_4) = \frac{\sum_{x_4} N(x_4)}{N_T}$$

Cloudy scenes are generated by a Monte Carlo method. This model enables one to build scenes containing rectangular *infinite* or *finite* clouds, made up of up to three layers. Convergence is ensured thanks to a great number of generated scenes. Random draws are performed to get the cloud layers properties values (altitude, thickness and optical depth), that are constrained by joint probability densities calculated from cloud occurrence climatology. A sensor is placed in the scene and optical transmission is calculated along its line of sight. Around 400 sensor positions are randomly chosen in order to cover the whole geographic area. In case of *finite* clouds, additional random draws are performed along the LOS, filling the scene with cloudy and clear-sky areas in agreement with cloud occurrence climatology and cloud length statistics. For *infinite* clouds the scene is either totally cloudy or totally clear.

Probability that a transmittance T is greater than a given threshold T_t is given by:

$$P(T \geq T_t) = \frac{\sum_k (T \geq T_t)}{\sum_k k} \quad (3)$$

where k stands for the different cloudy scenes realizations, $(T \geq T_t)$ is equal to 1 when the condition is fulfilled, 0 otherwise.

Based on the clouds joint probability densities (Eq. (1) in the *infinite* cloud case and Eq. (2) in the *finite* cloud case), sensor performances expressed as transmittance probabilities (Eq. (3)) can be determined.

3. SENSOR PERFORMANCES

Two main applications are considered to estimate detection performances: (1) a surveillance mission by an airborne electro-optical sensor firstly with a viewing angle close to the horizon and then with a more oblique viewing angle. (2) an optical link between a satellite and an airborne sensor, in nadir-viewing conditions.

3.1. Airborne surveillance sensor

The impact of cloud presence on airborne sensor performance is often translated in terms of CFLOS probabilities higher than a prescribed threshold P_T . This can be written as:

$$P(T=1) \geq P_T \quad (4)$$

where $P(T=1)$ is obtained from Eq. (3). In that case, clouds are considered as totally opaque.

Sensor performances are arbitrarily supposed not to be affected by cloud presence if $P_T \geq 0.95$. The lowest limit of the sensor field of view (FOV) θ_{min} (see Fig. 2 for description of observation geometry)

that will satisfy Eq. (4) with a prescribed P_T value can thus be determined by solving Eq. (4). Cloud layers are supposed to be horizontally infinitely wide in this first step.

This paper focuses on the Mediterranean area (17°N to 49°N and 3°W to 45°E). The airborne sensor altitude ranges between 12 and 20 km and the viewing angle ranges from -2.5° below the horizon up to 0° . Figure 3 displays the lowest limit of the sensor FOV (θ_{min}) as a function of the sensor altitude, for the four seasons, daytime, over the Mediterranean region such as $P(T=1) \geq 0.95$. θ_{min} strongly varies with sensor altitude. Best performances are achieved for highest sensor altitudes. For example, a sensor located at 19 km altitude or above has a probability of having a clear LOS higher than 0.95 whatever the season and LOS elevation angle, provided it is above -2.5° . On the other hand, below 13 km only few angles meet the requirements.

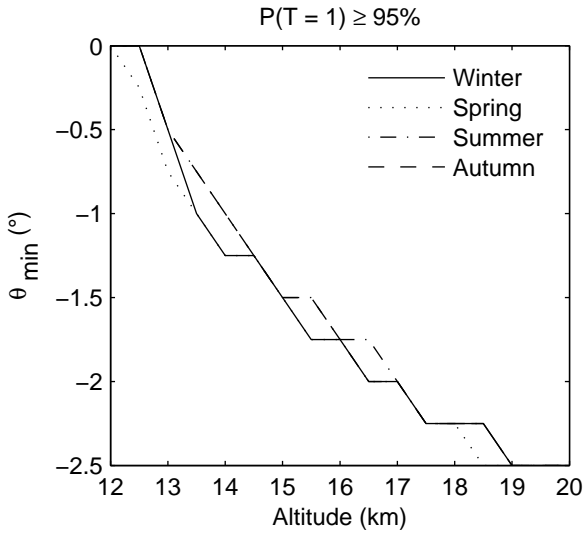


Figure 3. Lowest limit of the FOV θ_{min} to obtain a clear LOS probability higher than 95%. θ_{min} is given as a function of the sensor altitude, for the four seasons, by day, for the Mediterranean area. Clouds are considered to be infinitely horizontally wide. Cloud occurrences are obtained from CALIOP data.

These results are compared with sensor performance calculations presented in [9]. In this previous study, an analytical model based on mean cumulative probability distributions of high altitude cloud occurrences, with some simplifying hypotheses such as infinite and totally opaque clouds developed, was developed. The cloud climatology considered was obtained from 8-years of TOVS data [22][30] at a spatial resolution $1^\circ \times 1^\circ$. A comparison between high-clouds occurrences from TOVS data and CALIOP data is shown in Fig. 4, over the Mediterranean area at autumn season by day. CALIOP cloud occurrence can not be obtained with a spatial resolution as high as TOVS due to a lower revisit time and a shorter acquisition period. High-cloud occurrence from CALIOP is largely higher than TOVS, which is consistent with optical depth detection limits of each instrument: mean high-cloud occurrence over the

Mediterranean area from the TOVS climatology is close to 20% while it reaches 30% in CALIOP case.

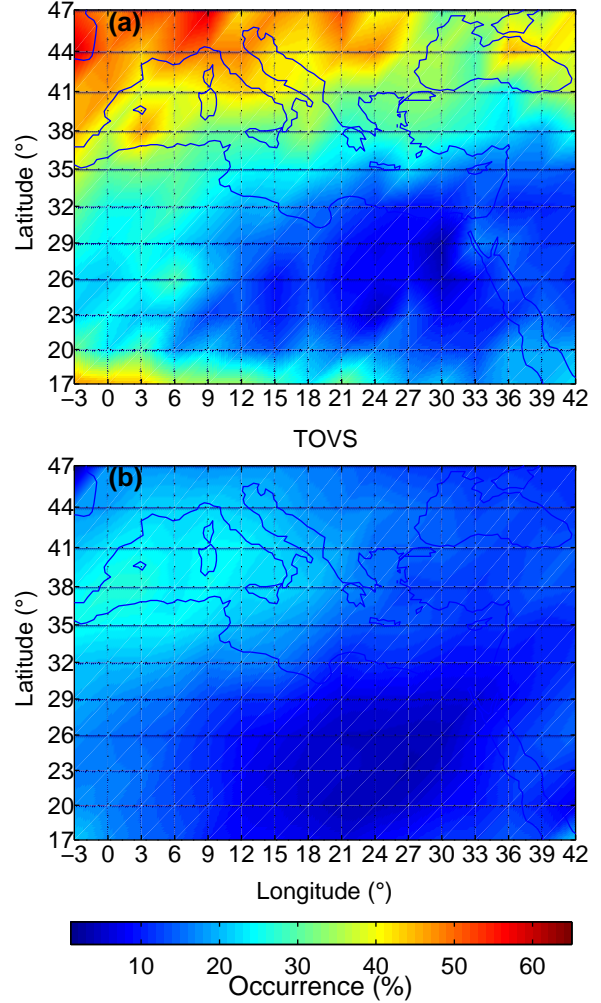


Figure 4. Comparison between high-clouds occurrences obtained over the Mediterranean area from CALIOP data (a) and TOVS data (b) at autumn season, whatever the cloud optical depth.

The lowest limit of the sensor FOV (θ_{min}) as a function of the sensor altitude obtained with TOVS cloud occurrence is presented in Fig. 5. It is important to notice that the choice of cloud climatology has an obvious influence on sensor performance calculations. Indeed, sensor performance calculated with CALIOP climatology is worse than the one obtained with the TOVS climatology. This is consistent with the lack of optically thin clouds in TOVS climatology which are included in CALIOP climatology. For example in summer, for a sensor altitude of 13 km, θ_{min} was evaluated to -1.6° with TOVS climatology against -0.75° with CALIOP climatology. More realistic finite rectangular clouds are taken into account, in order to improve sensor performance estimation. Transmittance statistics are computed considering Eq. (2). Sensor performance in term of the lowest limit of the sensor FOV as a function of the sensor altitude is shown in Fig. 6.

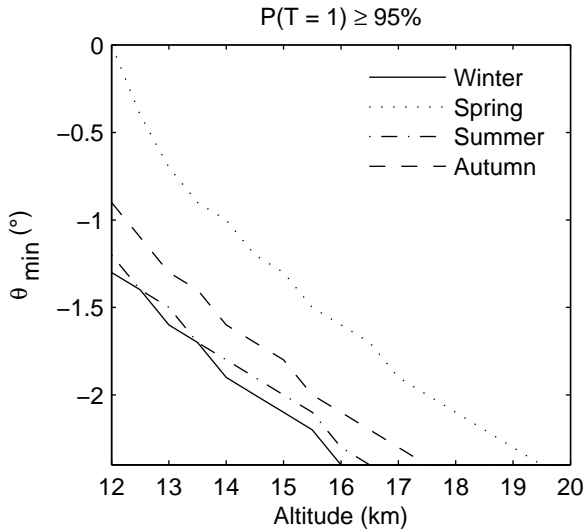


Figure 5. Same as Fig. 3 but with results from Chervet and Roblin (2006).

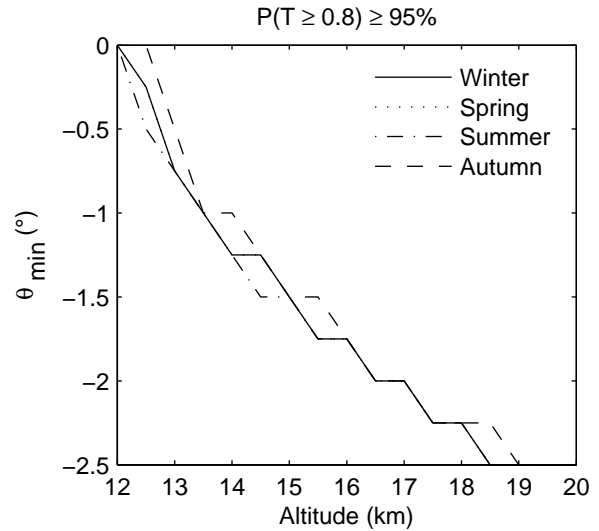


Figure 7. Same as Fig.3 but with transmittance threshold $T_t=0.8$ (instead of 1).

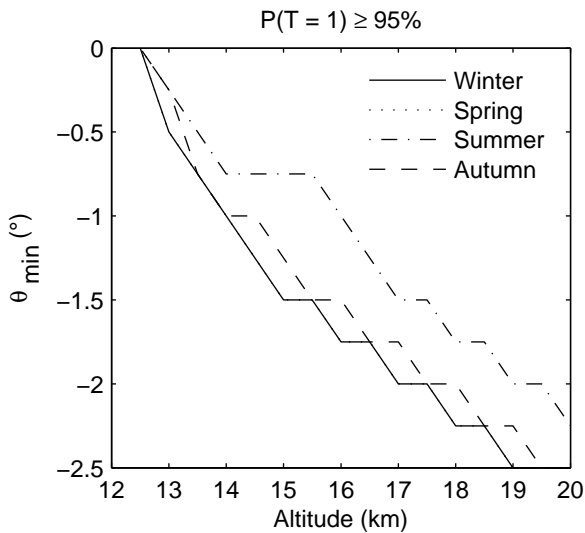


Figure 6. Same as Fig. 3 but with finite clouds.

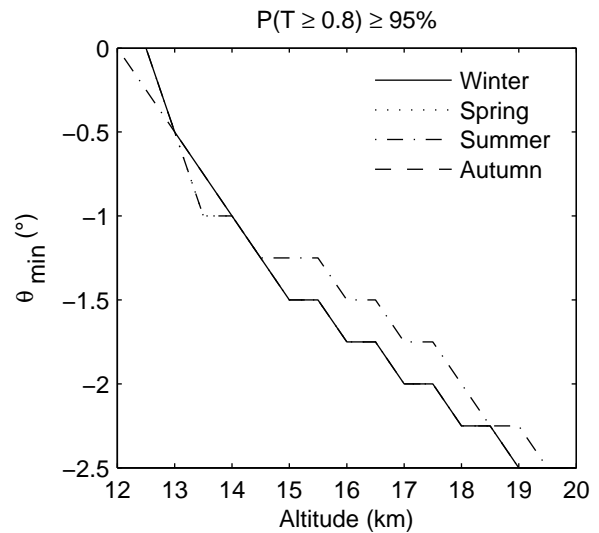


Figure 8. Same as Fig.7 but with finite clouds

In the main, it appears to be slightly worse than for *infinite* clouds except in summer where it is largely degraded. The performance degradation is in agreement with the lower probability of having a cloud-free LOS in the *finite* case compared to the *infinite* one. This trend is emphasized in summer when occurrence of clouds above 12 km from CALIOP climatology is more prominent than during the rest of the year.

Instead of evaluating CFLOS probabilities ($T_t=1$ in Eq. (3)), T_t can be lowered. A threshold $T_t=0.8$ has been chosen to calculate new sensor performance estimations. As previously, the lowest limit of the sensor FOV as a function of the sensor altitude is shown in Fig. 7 in case of *infinite* cloud and in Fig. 8 in case of *finite* cloud.

Performances reached with the new threshold are very close to those obtained with $T_t=1$. This trend can be understood by scrutinizing Fig. 9 showing histograms of transmittances values computed from the airborne surveillance sensor scenario. It can be noticed that most of the transmittances values are close to 0 (opaque cloud layer) or equal to 1 (cloud-free case). It is consistent with the close-to-the-horizon viewing conditions that lead to a large optical path inside the cloud and thus to a strong decrease in transmittance for a cloudy LOS. The great number of close-to-one transmittance values is in agreement with the high-cloud cover statistics estimated around only 30% at global scale with pronounced latitudinal variability ranging from 20% at mid-latitudes to more than 40% in the Tropics (Stubenrauch et al., 2006; Sassen et al., 2008).

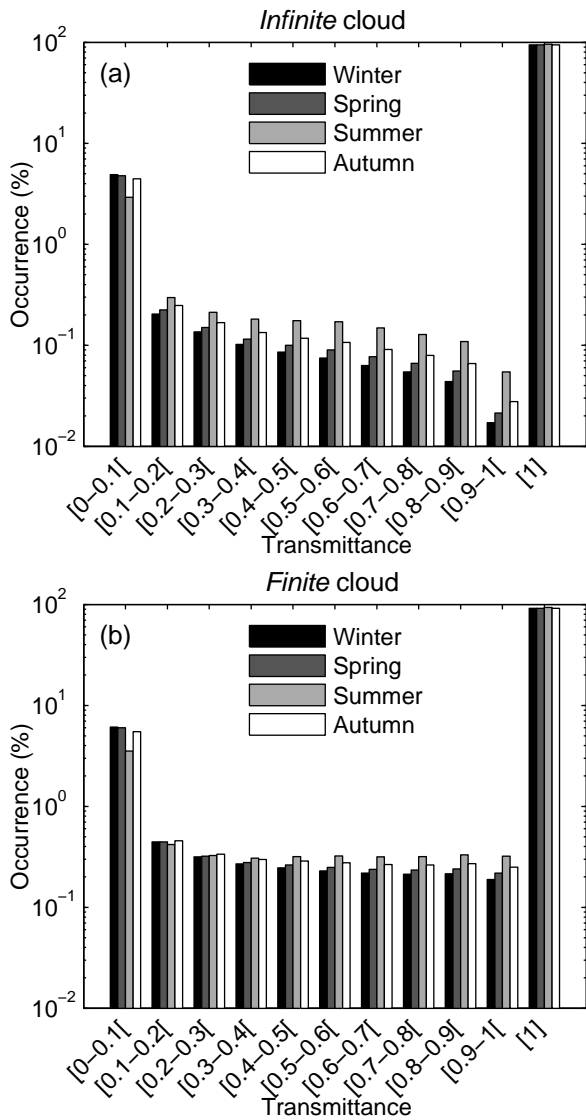


Figure 9. Normalized histogram of transmittance values, by season, in case of infinite cloud (a) and finite cloud (b). Transmittance are computed along the airborne sensor LOS with sensor altitude ranging between 12 and 20 km and viewing angle between -2.5° and 0° .

If we consider a wider viewing angle, the impact of the *finite* or *infinite* cloud model is more significant as can be observed in Fig. 10. The probability that the transmittance along the LOS is higher than a chosen threshold T_t is plotted relative to the threshold for the four seasons in the *infinite* and *finite* cloud cases. The sensor altitude is 20 km and the viewing angle is $\theta = -20^\circ$. The LOS is stopped at 7 km height in order to only consider the high-altitude clouds. For all seasons, the transmittance probability is higher in the *finite* cloud case than in the *infinite* one. In the case where the required performance is a transmittance probability higher than 0.8 with a threshold $T_t = 0.8$, only two configurations do not meet requirements: winter and spring with *infinite* cloud model.

In summary, performance of an airborne sensor with viewing angles close to the horizon can be estimated using the assumption of an infinitely wide and totally opaque cloud. The use of a more

sophisticated model with *finite* and non-opaque clouds does not change performances calculations a lot. When considering a lower viewing angle, the choice of the cloud model is more prominent.

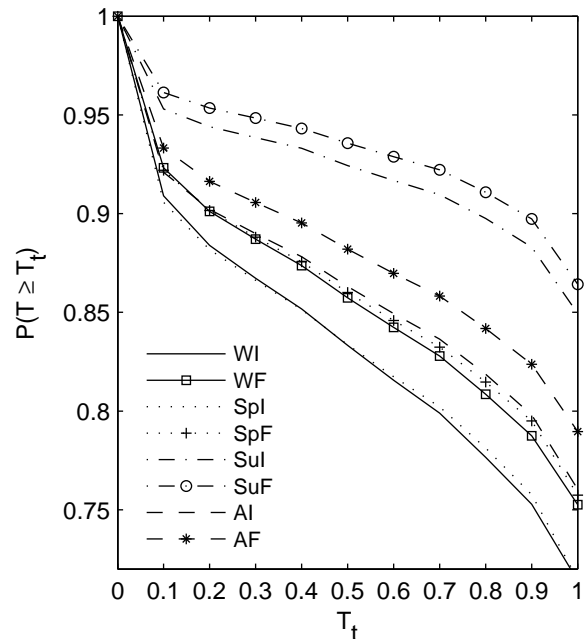


Figure 10. Probability of transmittance higher than the threshold T_t as a function of T_t . The airborne sensor is located at 20 km altitude with an oblique viewing angle $\theta = -20^\circ$. Transmittance probabilities are given for the Mediterranean area, by day, for the four seasons, in the infinite and finite clouds cases. Legend labels indicate season (W: Winter, Sp: Spring, Su: Summer, A: Autumn) and infinite (I) or finite (F) clouds cases.

3.2. Optical link between a satellite and an airborne sensor

Characterization of an optical link between a satellite and an airborne sensor also requires prediction of transmittance values. Transmittance computations are performed between a 600 km-altitude nadir-viewing satellite and an aircraft. The viewing geometry is given in Fig. 11. The probability that the transmittance along the LOS is higher than a chosen threshold T_t is calculated for six aircraft altitudes ranging between 9 and 14 km. Results are shown in Fig. 12 for the four seasons, with the *finite* cloud model and over the Mediterranean area. In the whole, transmittance probabilities obtained in winter, autumn and spring are very close. As in the previous case, they are higher in summer for the lowest aircraft altitudes because occurrences of clouds between 8 and 12 km are lower at this season. Probabilities of transmittances higher than T_t evenly decrease with the threshold. Nevertheless, occurrences of transmittances calculated with $T_t = 0.8$ are always above 0.9 whatever the season or the sensor altitude. If we suppose that optical link is not affected by cloud presence as soon as $P(T \geq 0.8) \geq 0.95$, aircraft has to be located above 10 km altitude in spring, autumn or winter.

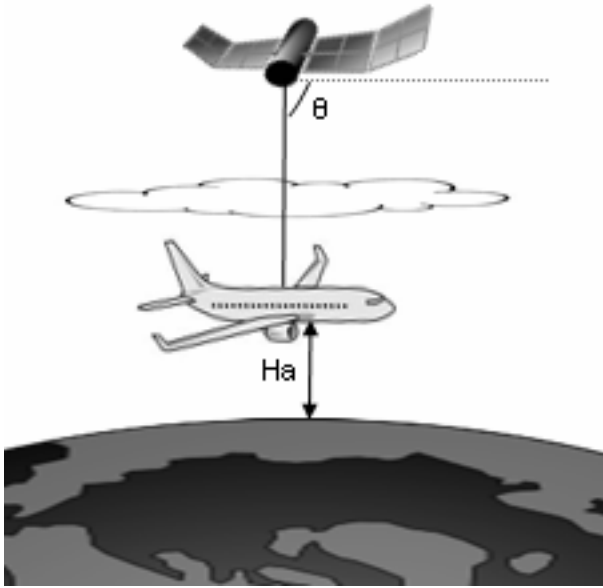


Figure 11. Viewing geometry of a satellite sensor establishing an optical link with an airborne sensor. Satellite height is $H=600$ km and is nadir viewing. The aircraft is located at altitude H_a .

In summer, whole altitudes present satisfactory performance. The threshold parameter and transmittance probability have been arbitrarily chosen. They have to be adapted in relation to expected applications. It should be interesting to repeat this study at different geographical locations in order to define the most promising area for airborne satellite optical link characterization.

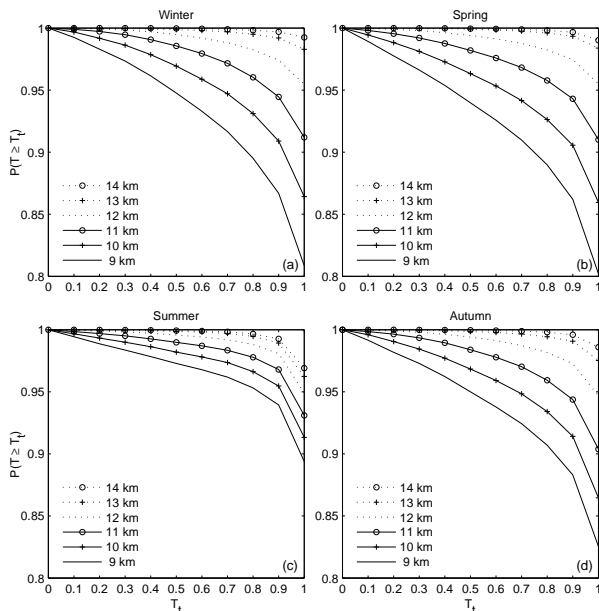


Figure 12. Probability of transmittance higher than the threshold T_t as a function of T_t . The satellite is located at 600 km altitude over the Mediterranean zone and is nadir viewing towards an airborne sensor whose altitude ranges from 9 to 14 km. Transmittance probabilities are given by day, in the finite clouds case, for the four seasons: Winter (a) Spring (b) Summer (c) Autumn (d).

4. CONCLUSION

Transmittance statistics along an airborne sensor LOS have been calculated based on a probabilistic approach to evaluate the sensor performance. A high-altitude cloud climatologic dataset was used to determine the impact of cloud presence along the LOS. CALIOP cloud products have been selected due to the detection limit of CALIOP instrument that allows the inclusion of non-opaque clouds, which were not previously taken into account in sensor performance studies. Different observation geometries have been considered in order to demonstrate the potential of the proposed method for various applications. In particular, close-to-the-horizon and oblique lines of sight were defined for airborne surveillance application and nadir LOS was chosen in case of optical link between a satellite and an airborne sensor. Results showed that assumption of horizontally infinitely wide opaque clouds is justified in the case of close-to-the-horizon lines of sight. As regards the other observation geometries, introduction of non-opaque clouds and a more realistic cloud model with a finite horizontal length may have a strong effect on performance estimation.

Clouds occurrences are strongly dependent on geographical location as well as cloud horizontal extent. Sensor performance is thus related to the sensor location. Prospects of this study will be to consider this geographical dependence in combination with seasonal variation in order to determine the best locations to place a sensor on globe or, on the contrary, zones to be avoided. Statistics of cloud length, restricted to a small area in this study, would give more precise transmittance estimations and thus more precise performance evaluations.

Acknowledgments

CALIPSO data were obtained from the NASA Langley Research Center Atmospheric Science Data Center. We thank the CALIPSO science team for providing these data.

5. REFERENCES

1. Liou K.-N., Y. Takano, S. C. Ou, A. Heymsfield, and W. Kreiss, 1990: Infrared transmission through cirrus clouds: A radiative model for target detection. *Appl. Opt.*, 29, 1886–1896.
2. Liou K.-N., Y. Takano, S. C. Ou and M. W. Johnson, 2000: Laser transmission through thin cirrus clouds. *Appl. Opt.*, 39, 4886–4894.
3. Ou S. C., Y. Takano, K. N. Liou, R. J. Lefevre, and M. W. Johnson, 2002: Laser transmission-backscattering through inhomogeneous cirrus clouds. *Appl. Opt.*, 41, 5744–5754.
4. Shields J. E., A. R. Burden, R. W. Johnson, M. E. Karr and J. G. Baker, 2005: New cloud free line of sight statistics measured with digital

whole sky imager. Proceedings, *SPIE* Vol 5891, 58910M.

doi:10.1175/2010BAMS3009.1

5. Lund I. A. and M. D. Shanklin, 1972: Photogrammetrically Determined Cloud-Free Lines-Of-Sight through the Atmosphere. *J. Appl. Meteor.*, 11:773-782.
6. Lund I. A. and M. D. Shanklin, 1973: Universal Methods for Estimating Probabilities of Cloud-Free Lines-Of-Sight Through the atmosphere. *J. Appl. Meteor.*, 12:28-35.
7. Lund I. A., D. D. Grantham and R. E. Davis, 1980: Estimating probabilities of Cloud-Free Fields-of-View from the Earth through the atmosphere. *J. Appl. Meteor.*, 19:452-463.
8. Hobbs R., J. Mitchell, M. A. Bedrick, D. J. Rusk and R. L. Rose, 2003: Use of satellite climatology for assessing cloud-free-line-of-sight probabilities, Preprints, *12th Conference on Satellite Meteorology and Oceanography, Long Beach, CA, Amer. Meteor. Soc.*, P1.1.
9. Chervet P. and A. Roblin, 2006: High altitude cloud effects on airborne electro-optical sensor performances. *J. Atmos. Oceanic Technol.*, 23, 11, 1530-1538.
10. Stubenrauch C. J., A. Chedin, G. Radel, N. A. Scott and S. Serrar, 2006: Cloud properties and their seasonal and diurnal variability from TOVS Paths-B. *J. Climate*, 5531-5553.
11. Wylie D. P. and W. P. Menzel, 1999: Eight years of high cloud statistics using HIRS. *J. Climate* 12, 170-184.
12. Wylie D. P., W. P. Menzel, H. M. Woolf and K. I. Strabala, 1994: Four years of global cirrus cloud statistics using HIRS. *J. Climate*, 7, 1972-1986.
13. Stephens G. L., D.G. Vane, R.J. Boain, G.G. Mace, K. Sassen, Z.E. Wand, A.J. Illingworth, E.J., O'Connor, W.B. Rossow, S.L. Durden, S. Miller, R.T. Austin, A. Benedetti, and C. Mitrescu, 2002: The CloudSat mission and the A-train. A new dimension of space-based observations of clouds and precipitation, *Bull. Amer. Meteor. Soc.*, 83, 1771-1790.
14. Winker D. M., W. H. Hunt, and M. J. McGill, 2007: Initial performance assessment of CALIOP. *Geophys. Res. Lett.*, 34, L19803, doi:10.1029/2007GL030135.
15. Winker D. M., Mark A. Vaughan, Ali Omar, Yongxiang Hu, Kathleen A. Powell, Zhaoyan Liu, William H. Hunt, Stuart A. Young, 2009: Overview of the CALIPSO Mission and CALIOP Data Processing Algorithms. *J. Atmos. Oceanic Technol.*, 26, 2310–2323.
16. Winker D. M. and 18 coauthors, 2010: The CALIPSO Mission: a global 3D view of aerosols and clouds, *B. Am. Meteorol. Soc.*, 91, 1211-1229,
17. Hunt W. H., D. M. Winker, M. A. Vaughan, K. A. Powell, P. L. Luckner and C. Weimer, 2009: CALIPSO Lidar description and performance assessment, *J. Atmos. Oceanic Technol.*, 26, 1214-1228, doi:10.1175/2009JTECHA1223.1.
18. Dupont J.-C., M. Haeffelin, Y. Morille, V. Noël, P. Keckhut, D. Winker, J. Comstock, P. Chervet and A. Roblin, 2010: Macrophysical optical properties of midlatitude cirrus clouds from ground-based lidars and collocated CALIOP observations. *J. Geophys. Res.*, 115, doi:10.129/2009JD011943.
19. Ackerman S. A., R. E. Holz, R. Frey, E. W. Eloranta, B. Madux and M. McGill, 2008: Cloud detection with MODIS: Part II validation. *J. Atmos. Oceanic Technol.*, 25, 1073-1086, doi:10.1175/2007JTECHA1053.1.
20. Rossow W. B. and R. A. Schiffer, 1999: Advances in understanding clouds from ISCCP. *Bull. Am. Meteorol. Soc.*, 80, 2261-2286, doi :10.1175/1520-0477.
21. Liao X., W. B. Rossow and D. Rind, 1995: Comparison between SAGE II and ISCCP cloud amounts. *J. Geophys. Res.*, 100, 1121-1135.
22. Scott N. A., A Chédin, R. Armante, J. Francis, C. Stubenrauch, J. –P. Chaboureau, F. Chevallier, C. Claud and F. Cheruy, 1999: Characteristics of the TOVS Pathfinder Path-B Dataset. *Bull. Amer. Meteor. Soc.* 80, 2679-2701.
23. Wylie D. P., P. Piironen, W. Wolf and E. Eloranta, 1995: Understanding satellite cirrus cloud climatologies with calibrated lidar optical depths. *J. Atmos. Sci.*, 52, 4327-4343.
24. Sassen K. and B. S. Cho, 1992: Subvisual-thin cirrus lidar dataset for satellite verification and climatological research. *J. Appl. Meteor.*, 31, 1275-1285.
25. Davis, S., and Coauthors, 2010: In situ and lidar observations of tropopause subvisible cirrus clouds during TC4. *J. Geophys. Res.*, 115, D00J17, doi:10.1029/2009JD013093.
26. Noel V. and M. Haeffelin, 2007: Midlatitude cirrus clouds and multiple tropopause from a 2002-2006 climatology over the SIRTAs observatory. *J. Geophys. Res.*, 112, D13206, doi:10.1029/2006JD007753.
27. Keckhut P., F. Borchi, S. Bekki, A. Hauchecorne and M. SiLiaouina, 2006: Cirrus Classification at midlatitude from systematic lidar observations. *J. Appl. Meteorol. Climatol.*, 45, 249-258.
28. Comstock J. M., TP. Ackerman, and G.G. Mace, 2002: Ground-based lidar and radar remote sensing of tropical cirrus clouds at

Nauru Island: cloud statistics and radiative impact, *J. Geophys. Res.*, 107, 4714.

29. Sassen K., Z. Wang and D. Liu, 2008: The global distribution of cirrus clouds from CloudSat/CALIPSO measurements, *J. Geophys. Res.* 113, D00A12, doi:10.1029/2008JD009972.
30. Rogers, R. R., and Coauthors, 2011: Assessment of the CALIPSO Lidar 532nmattenuated backscatter calibration using the NASA LaRC airborne High Spectral Resolution Lidar. *Atmos. Chem. Phys.*, 11, 1295–1311, doi:10.5194/acp-11-1295-2011.
31. Vaughan, M, A., K. A. Powell, D. M. Winker, C. A. Hostetler, R. E. Kuehn, W. H. Hunt, B. J. Getzewich, S. A. Young, Z. Liu, and M. J. McGill, 2009: Fully automated detection of cloud and aerosol layers in the CALIPSO lidar measurements, *J. Atmos. Oceanic Technol.*, 26(10), 2034-2050, doi:10.1175/2009JTECHA1228.1.
32. Powell, K., and Coauthors, 2011: Cloud–Aerosol Lidar Infrared Pathfinder Satellite Observations Data Management System: Data products catalog. Doc. PC-SCI-503, Release 3.4, NASA Langley Research Center, 99 pp. [Available online at http://www.calipso.larc.nasa.gov/products/CALIPSO_DPC_Rev3x4.pdf.]
33. Thorsen T.J., Q. Fu, and J. Comstock, 2011: Comparison of the CALIPSO satellite and ground-based observations of cirrus clouds at the ARM TWP sites. *J. Geophys. Res.*, 116, D21203, doi:10.1029/2011JD015970 (2011).
34. Yorks, J. E., D. L. Hlavka, M. A. Vaughan, M. J. McGill, W. D. Hart, S. Rodier, and R. Kuehn (2011): Airborne validation of cirrus cloud properties derived from CALIPSO lidar measurements: Spatial properties, *J. Geophys. Res.*, 116, D19207, doi:10.1029/2011JD015942.
35. Dupont J. C., 2008: Impact des nuages haute altitude sur le bilan radiatif à la surface de la terre : quantification expérimentale et analyse. *PhD Thesis Ecole Polytechnique*, 206 pp.
36. Stubenrauch C. J., W. B. Rossow, F. Chérub, A. Chédin and N. A. Scott, 1999: Clouds as seen by satellite sounders (3I) and imagers (ISCCP). Part I: Evaluation of cloud parameters. *J. Climate*, 12, 2189-2213.